Electronic Supplementary Material (ESI) for Dalton Transactions.
This journal is © The Royal Society of Chemistry 2024

Electronic Supplementary Information (ESI)

Harnessing Plasma-generated Reactive Species for the Synthesis of Different Phases of Molybdenum Oxide to Study Adsorption and Photocatalytic Activity

Parismita Kalita[a, b], Palash Jyoti Boruah[a], A. R. Pal[a, b] and H. Bailung[a, b, c, *]

[a] Plasma Application Laboratory, Physical Sciences Division, Institute of Advanced Study in Science and Technology (IASST), Paschim Boragaon, Guwahati – 781035, Assam, India

[b] Academy of Scientific and Innovative Research (AcSIR), Ghaziabad, Uttar Pradesh – 201002, India

[c] Department of Physics, Bodoland University, Kokrajhar – 783370, Assam, India

[*]*E-mail: hbailung@yahoo.com*

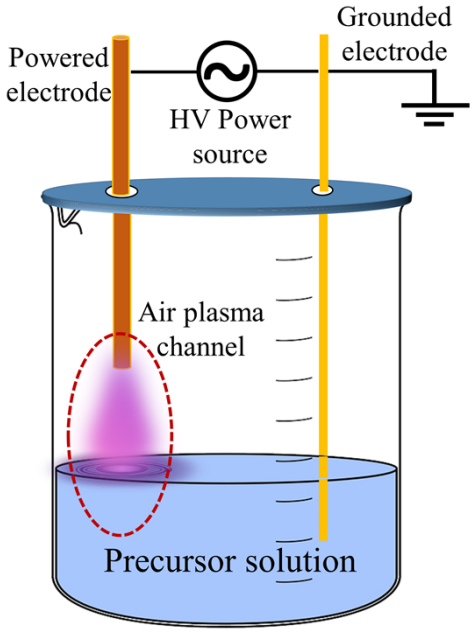

Fig. S1. Schematic representation of the plasma liquid reactor which shows the generation of atmospheric pressure air plasma channel above the Mo precursor solution.

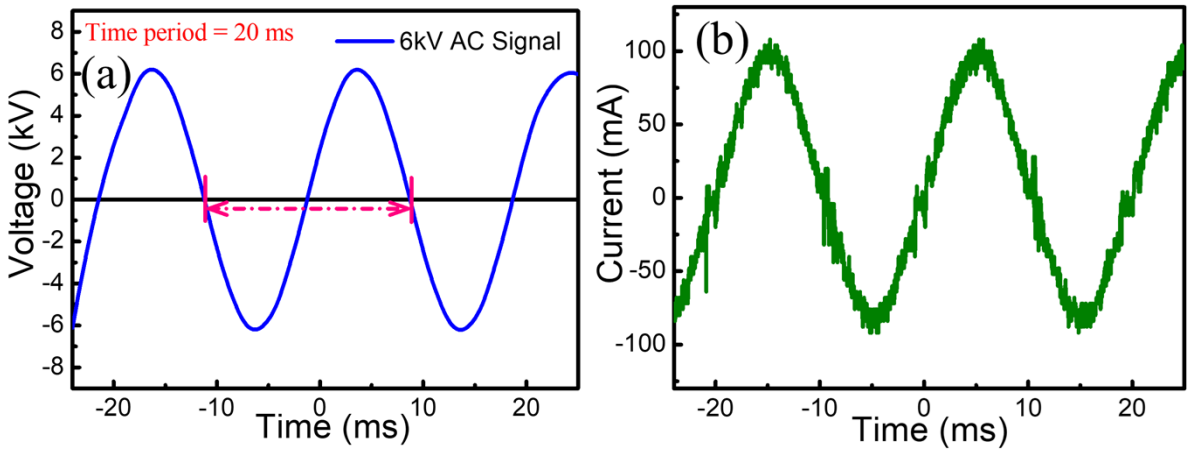

Fig. S2. Typical instantaneous (a) applied AC voltage signal waveform and (b) the corresponding discharge current signal.

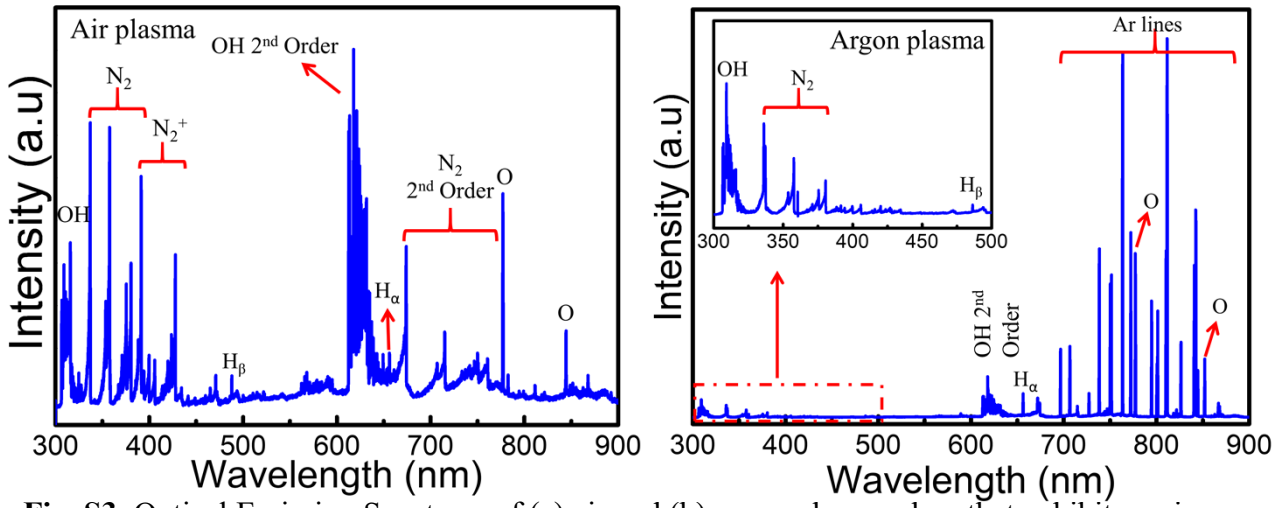

Fig. S3. Optical Emission Spectrum of (a) air and (b) argon plasma glow that exhibits various reactive species in the discharge zone.

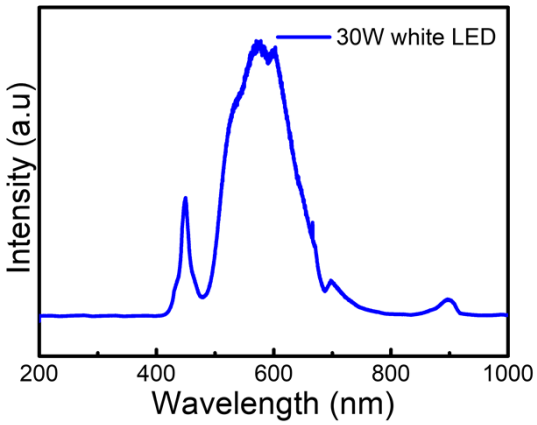

Fig. S4. Optical Emission Spectrum (OES) of 30W white LED.

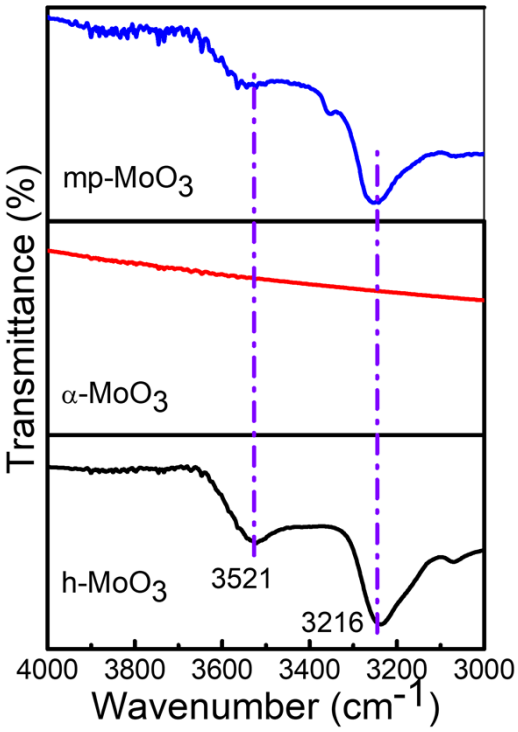

Fig. S5. FTIR spectra of three different phases of molybdenum oxide in the spectral range between 4000-3000 cm^{-1}.

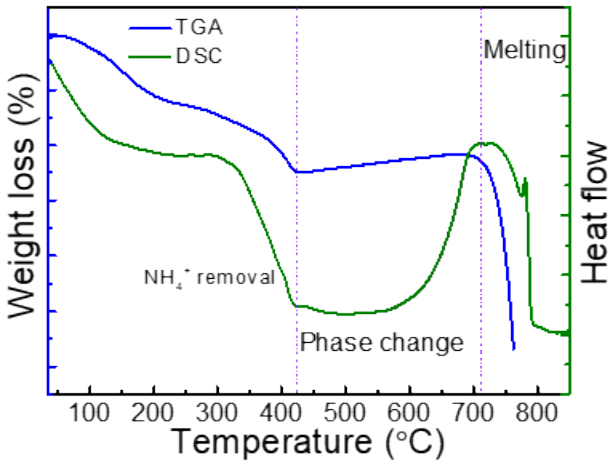

Fig. S6. TGA and DSC thermograms for h-MoO_3 sample from room temperature to 850 °C.

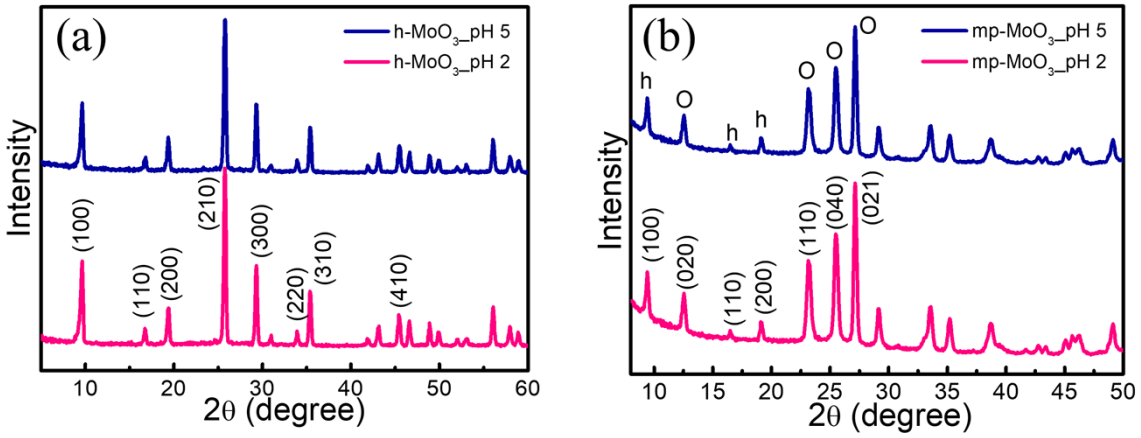

Fig. S7. XRD pattern of (a) h-MoO_3 and (b) mp-MoO_3 synthesized at different initial pH of the precursor solution.

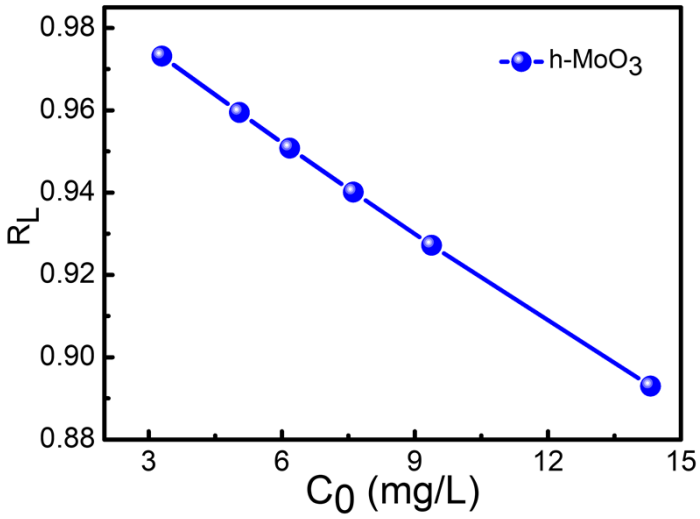

Fig. S8. The dimensionless parameter (R_L) defined from the Langmuir isotherm model.

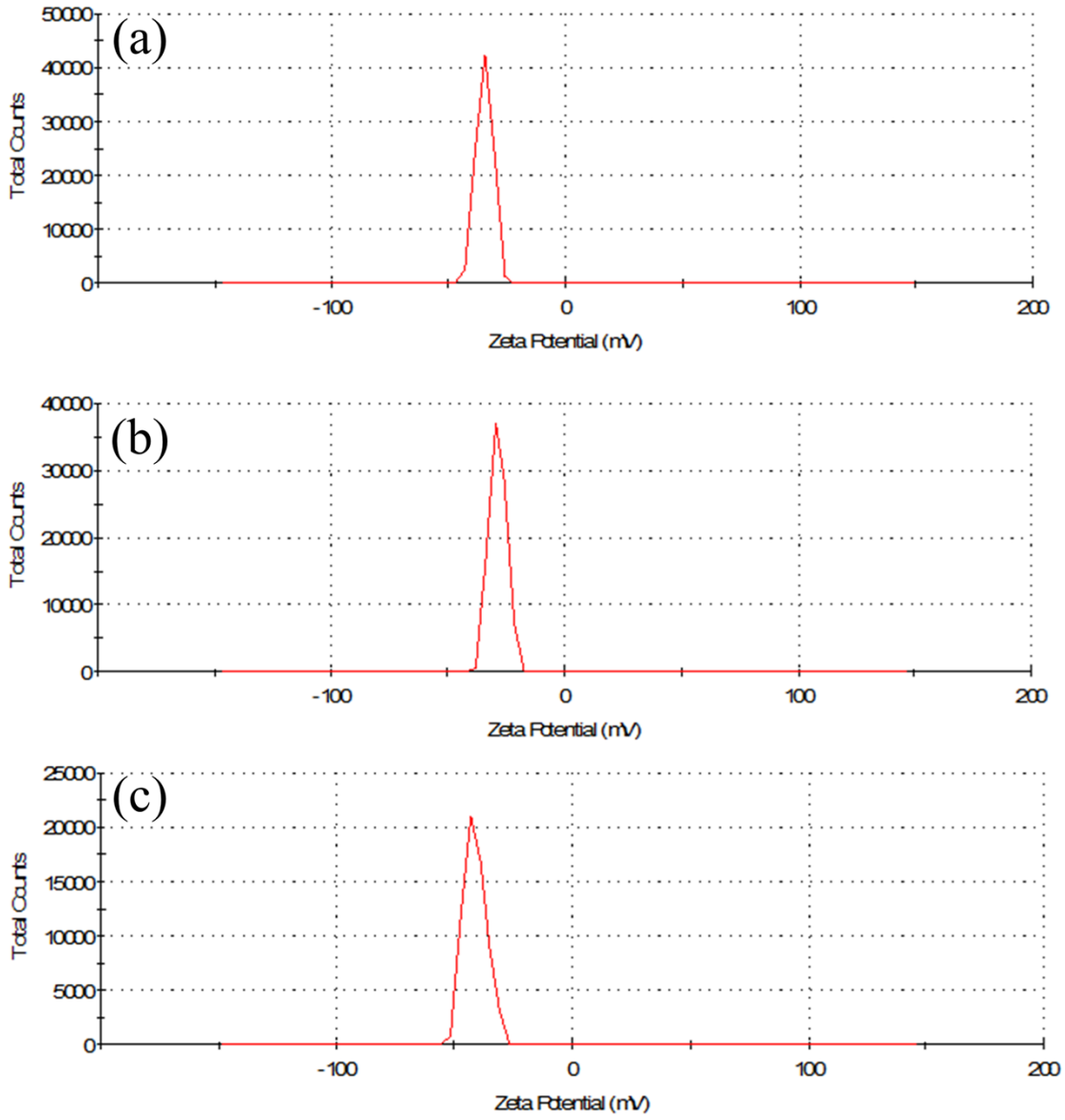

Fig. S9. Zeta potential measurement for the three different phases of molybdenum oxide.

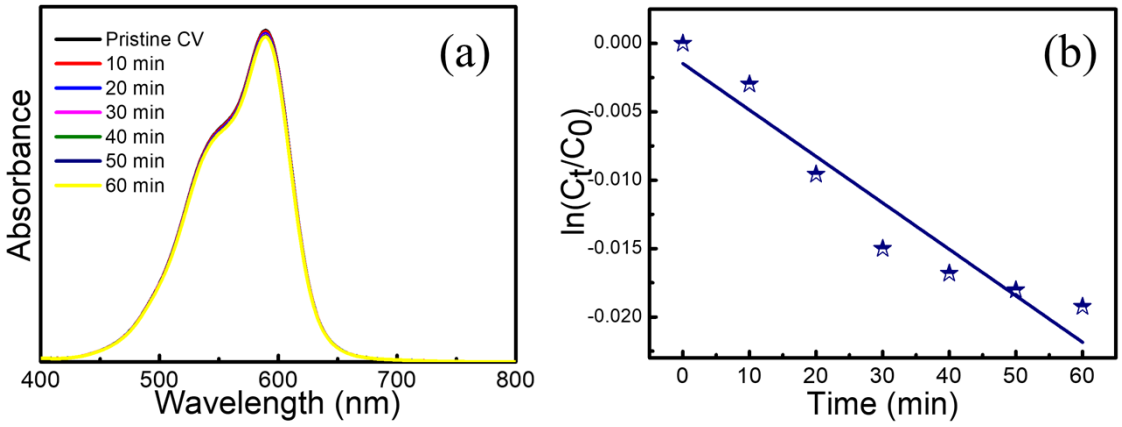

Fig. S10. (a) Photo-degradation spectra of CV dye molecules without loading any catalyst as a control experiment for dye degradation and the corresponding (b) pseudo-first-order rate kinetics.

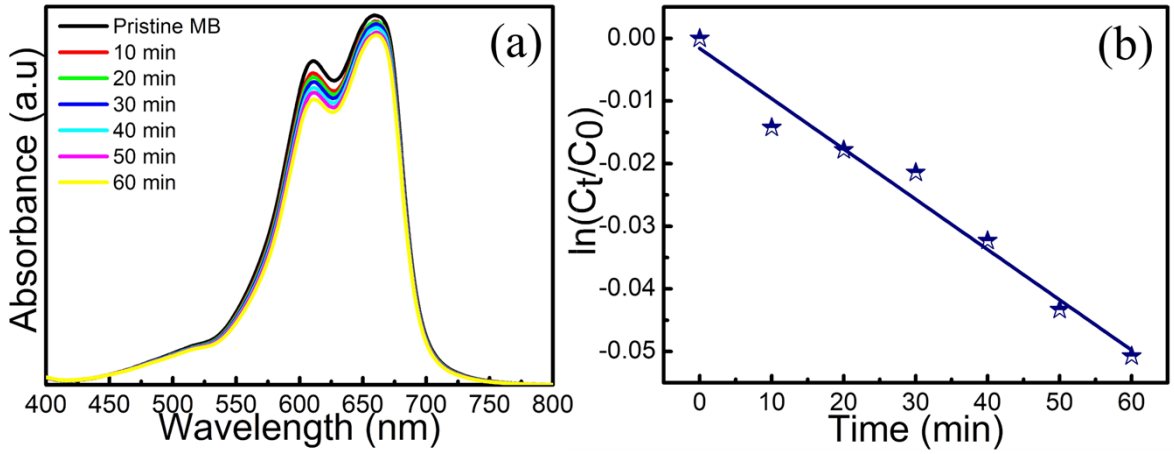

Fig. S11. (a) Photo-degradation spectra of MB dye molecules without loading any catalyst as a control experiment for dye degradation and the corresponding (b) pseudo-first-order rate kinetics.

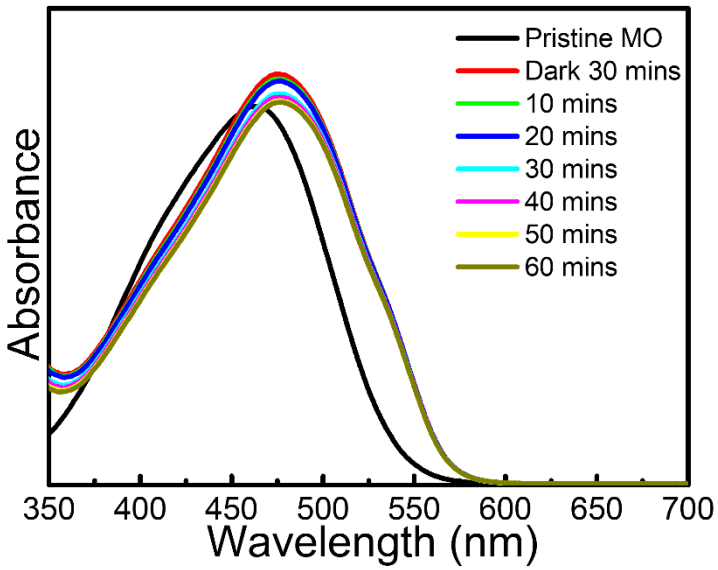

Fig. S12. UV-Vis photo-degradation spectra of Methyl orange dye molecules using h-MoO_3 sample under visible light illumination.

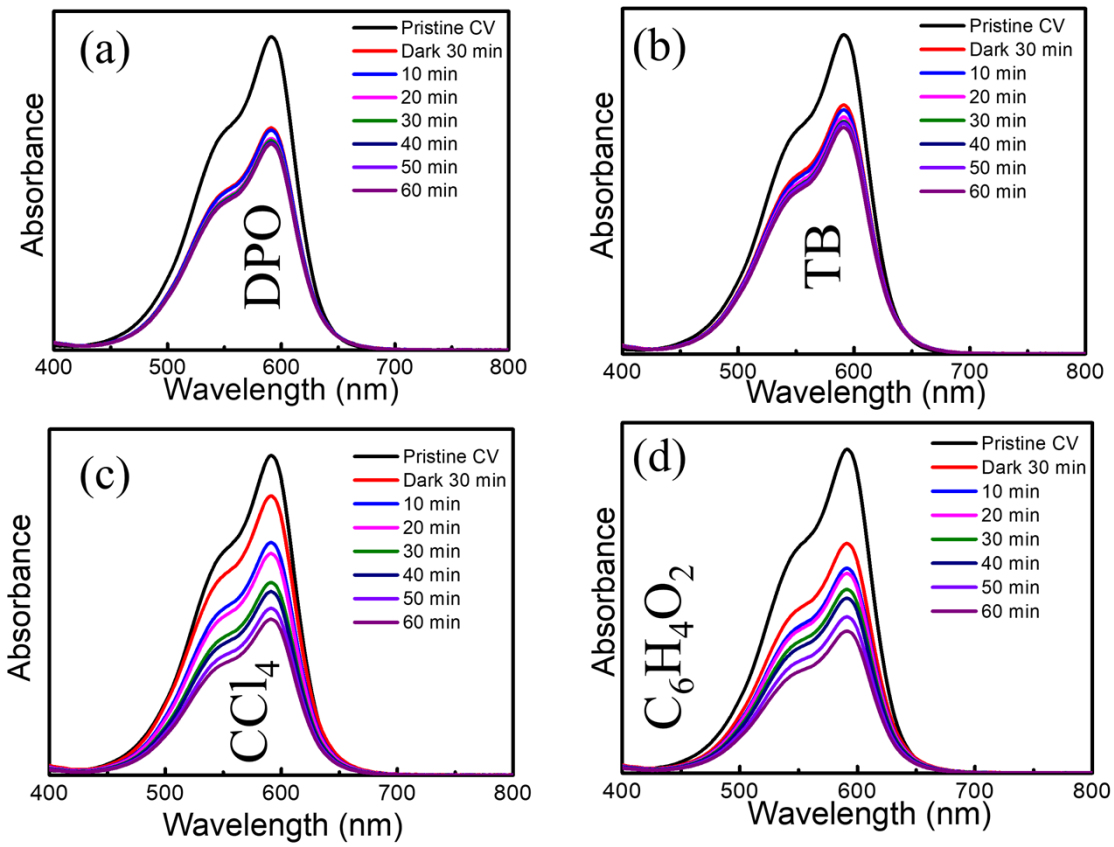

Fig. S13. Photo-degradation UV-Vis absorption spectra of CV dye molecules upon 60 mins of visible light irradiation in the presence of (a) di-potassium oxalate ($K_2C_2O_4.H_2O$), (b) *tert*-butanol ($(CH_3)_3OH$), (c) carbon tetrachloride (CCl_4), and (d) *p*-benzo-quinone ($C_6H_4O_2$).

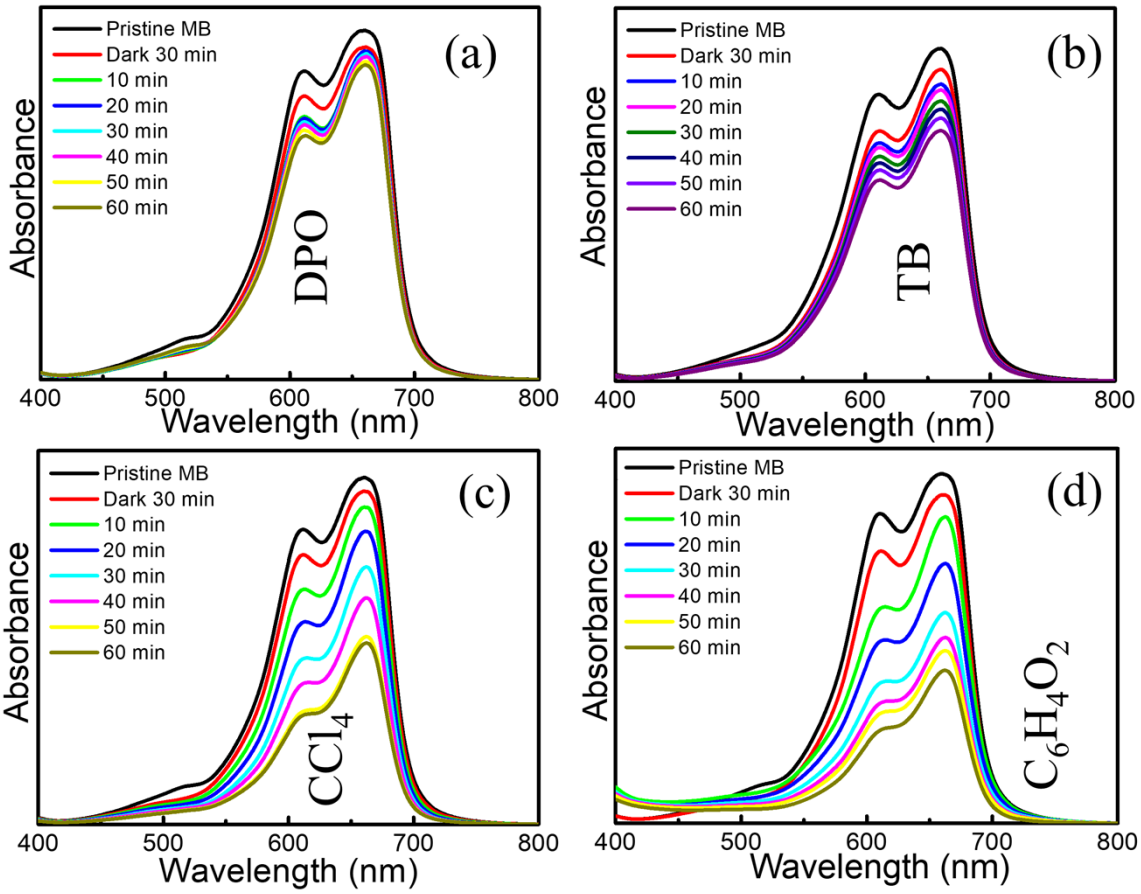

Fig. S14. Photo-degradation UV-Vis absorption spectra of MB dye molecules upon 60 mins of visible light irradiation in the presence of (a) di-potassium oxalate ($K_2C_2O_4.H_2O$), (b) *tert*-butanol ($(CH_3)_3OH$), (c) carbon tetrachloride (CCl_4), and (d) *p*-benzo-quinone ($C_6H_4O_2$).

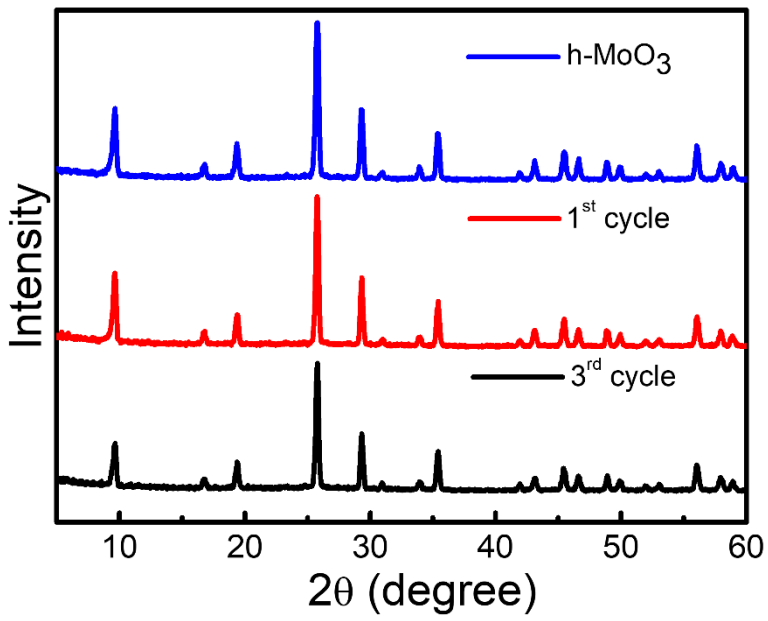

Fig. S15. XRD pattern of the photocatalyst before and after reuse during recycling procedure.

Table S1: A comparison table of different procedures employed for the synthesis of different phases of molybdenum oxide

Material	Synthesis procedure	Source of nanomaterial	Phase/Shape	Application	Reference
MoO_x	Solution plasma	Mo electrode	Mixed phase of MoO_3, MoO_2, and Mo_4O_{11} Elongated plate-like	Adsorption and Photocatalysis	[1]
MoO_x	Atmospheric pressure glow discharge	Mo electrode	Mixed phase of MoO_3, MoO_2, and Mo_4O_{11} Nanocylinders and prisms	Photocatalysis	[2]
MoO_x	Atomic layer deposition	$Mo(CO)_6$	Mixed phase of	-	[3]
MoO_x	Spark-plasma	MoO_3 + Mo powder mixture	Mixed phase of α-MoO_3, MoO_2, γ-MoO_3, $Mo_{17}O_{47}$, $Mo_{18}O_{52}$	-	[4]
MoO_x	Plasma-enhanced hot filament chemical vapor deposition	MoO_3 powder	Mixed phase of MoO_2 and Mo_4O_{11}	-	[5]

h-MoO_3 α-MoO_3 mp-MoO_3	Air plasma Air plasma+Calcination Argon plasma	Ammonium heptamolybdate tetrahydrate	Single-phase and hexagonal microrods Single-phase and microsheet-like structure Mixed phase of both hexagonal and orthorhombic phase and irregular cluster	Adsorption and Photocatalysis	This work

Table S2: Formation of molybdenum oxides at different pH of the initial precursor solution and the corresponding phase of the material

Precursor solution	**Plasma**	**pH of the initial solution**	**pH of the plasma-treated solution**	**Treatment time**	**Phase of the material**
AHM	Air plasma	2.0	1.24	45 mins	Hexagonal
AHM	Air plasma	5.0	2.1	120 mins	Hexagonal
AHM	Air plasma	7.0	5.43	120 mins	No precipitation
AHM	Air plasma	10.0	9.14	120 mins	No precipitation
AHM	Argon plasma	2.0	1.74	120 mins	Hexagonal and Orthorhombic

AHM	Argon plasma	5.0	3.95	120 mins	Hexagonal and Orthorhombic
AHM	Argon plasma	7.0	6.55	120 mins	No precipitation
AHM	Argon plasma	10.0	9.42	120 mins	No precipitation

Table S3: Fitted adsorption kinetic parameters of the pseudo-first-order kinetic model, pseudo-second-order kinetic model, and inter-particle diffusion model

Sample	$Q_{e(exp)}$ (mg/gm)	Pseudo-first-order			Pseudo-second-order			Inter-particle diffusion model		
		$Q_{e(cal)}$ mg/gm	k_1 min^{-1}	R^2	$Q_{e(cal)}$ mg/gm	k_2 gm/mg/ min^{-1}	R^2	C_i mg/gm	k_i gm/mg/ $min^{1/2}$	R^2
h-MoO_3	33.25	16.31	0.096	0.82	29.50	1.435	0.99	23.07	1.822	0.88
mp-MoO_3	62.54	44.23	0.051	0.87	50.86	0.443	0.98	22.10	4.957	0.95

Table S4: Fitted parameters of different isotherm models for the adsorption of CV dye molecules onto h-MoO_3 and mp-MoO_3 as an adsorbate

Isotherm model	Parameters	h-MoO_3	mp-MoO_3
Langmuir	Q_{max}	500.00 mg/gm	757.47mg/gm
	K_L	8.37 mL/mg	6.68 mL/mg
	R^2	0.99650	0.93943
Freundlich	1/n	1.03	0.96
	K_f	4.21 L/mg	5.19 L/mg
	R^2	0.99674	0.98959
Dubinin-Radushkevich	Q_{max}	49.56 mg/gm	66.21 mg/gm
	β	15.19 mol^2/kJ^2	17.90 mol^2/kJ^2
	E	0.18 kJ/mol	0.17 kJ/mol
	R^2	0.81343	0.77111
Sips	1/n	1.10	1.02

	K_s	0.00786	0.00645
	R^2	0.99772	0.98794

References:

[1] A. Khlyustova, N. Sirotkin, A. Kraev, V. Titov, A. Agafonov, Plasma-liquid synthesis of MoOxand WO3as potential photocatalysts, Dalt. Trans. 49 (2020) 6270–6279. https://doi.org/10.1039/d0dt00834f.

[2] N. Sirotkin, A. Khlyustova, V. Titov, A. Agafonov, Plasma-assisted synthesis and deposition of molybdenum oxide nanoparticles on polyethylene terephthalate for photocatalytic degradation of rhodamine B, Plasma Process. Polym. 17 (2020) 1–13. https://doi.org/10.1002/ppap.202000012.

[3] P.C. Juan, K.C. Lin, W.H. Cho, C.C. Kei, W.H. Hung, H.P. Shi, Plasma-enhanced atomic layer deposition of molybdenum oxides using molybdenum hexacarbonyl as the precursor, Mater. Chem. Phys. 288 (2022) 126395–126404. https://doi.org/10.1016/j.matchemphys.2022.126395.

[4] F. Kaiser, M. Schmidt, Y. Grin, I. Veremchuk, Molybdenum Oxides MoO x: Spark-Plasma Synthesis and Thermoelectric Properties at Elevated Temperature, Chem. Mater. 32 (2020) 2025–2035. https://doi.org/10.1021/acs.chemmater.9b05075.

[5] B.B. Wang, X.L. Qu, M.K. Zhu, Y.A. Chen, K. Zheng, X.X. Zhong, U. Cvelbar, K. Ostrikov, Plasma produced photoluminescent molybdenum sub-oxide nanophase materials, J. Alloys Compd. 765 (2018) 1167–1173. https://doi.org/10.1016/j.jallcom.2018.06.279.